BBA - Proteins and Proteomics 1872 (2024) 140992

Contents lists available at ScienceDirect

BBA - Proteins and Proteomics

journal homepage: www.elsevier.com/locate/bbapap

Research Paper

Characterisation of the forest cobra (*Naja melanoleuca*) venom using a multifaceted mass spectrometric-based approach

C. Ruth Wang [a], Alix C. Harlington [b], Marten F. Snel [a,c], Tara L. Pukala [a,*]

[a] Discipline of Chemistry, School of Physics, Chemistry and Earth Sciences, The University of Adelaide, Adelaide 5005, Australia
[b] Department of Molecular and Biomedical Science, School of Biological Sciences, The University of Adelaide, Adelaide 5005, Australia
[c] Proteomics, Metabolomics and MS-Imaging Core Facility, South Australian Health and Medical Research Institute, Adelaide 5005, Australia

ARTICLE INFO

Keywords:
Snake venom proteins
Forest cobra
Proteomics
Mass spectrometry

ABSTRACT

Snake venoms consist of highly biologically active proteins and peptides that are responsible for the lethal physiological effects of snakebite envenomation. In order to guide the development of targeted antivenom strategies, comprehensive understanding of venom compositions and in-depth characterisation of various proteoforms, often not captured by traditional bottom-up proteomic workflows, is necessary. Here, we employ an integrated 'omics' and intact mass spectrometry (MS)-based approach to profile the heterogeneity within the venom of the forest cobra (*Naja melanoleuca*), adopting different analytical strategies to accommodate for the dynamic molecular mass range of venom proteins present. The venom proteome of *N. melanoleuca* was catalogued using a venom gland transcriptome-guided bottom-up proteomics approach, revealing a venom consisting of six toxin superfamilies. The subtle diversity present in the venom components was further explored using reversed phase-ultra performance liquid chromatography (RP-UPLC) coupled to intact MS. This approach showed a significant increase in the number of venom proteoforms within various toxin families that were not captured in previous studies. Furthermore, we probed at the higher-order structures of the larger venom proteins using a combination of native MS and mass photometry and revealed significant structural heterogeneity along with extensive post-translational modifications in the form of glycosylation in these larger toxins. Here, we show the diverse structural heterogeneity of snake venom proteins in the venom of *N. melanoleuca* using an integrated workflow that incorporates analytical strategies that profile snake venom at the proteoform level, complementing traditional venom characterisation approaches.

1. Introduction

Snakebite envenomation is classed as a 'neglected tropical disease' by the World Health Organisation (WHO) that claims 2.7 million victims annually worldwide, with up to 138, 000 reported deaths and the majority of snakebite survivors permanently debilitated [1–3]. The morbidity and mortality attributed to snakebite envenomation are largely due to the potent nature of snake venom. Venom is a complex mixture of enzymatic and non-enzymatic toxins that act synergistically to disrupt various physiological pathways in the body. The effects of these proteins often result in tissue necrosis, neuromuscular paralysis, systemic haemorrhage and eventual death [4–9].

Antivenom treatment remains the current cornerstone therapy for snakebite envenomation where animal-derived antibodies raised against a specific snake venom are administered [8,10]. However, due to the variable nature of production, animal-based antivenoms are not always efficacious and can often fail to prevent key toxins from eliciting toxicity, leading to permanent debilitation in snakebite victims despite

Abbreviations: MS, mass spectrometry; PTMs, post translational modifications; BU proteomics, bottom-up proteomics; MP, mass photometry; SEC, size exclusion chromatography; SDS-PAGE, sodium dodecyl-sulphate polyacrylamide gel electrophoresis; RP-UPLC, reversed phase-ultra performance liquid chromatography; 3FTx, three finger toxin; SVMP-DIS, snake venom metalloproteinase and disintegrin; SVSP, snake venom serine protease; PDE, phosphodiesterase; CTL, C-type lectin; NP, natriuretic peptide; KUN, kunitz-type serine protease inhibitor; PLA_2, phospholipase A_2; LAAO, L-amino acid oxidase; CYS, cystatin; 5'NUC, 5'nucleotidase; CVF, cobra venom factor; AP, aminopeptidase; SVSP INH, snake venom serine protease inhibitor; HYAL, hyaluronidase; HYD, hydrolase; PLA_2 INH, phospholipase A_2 inhibitor; CRiSP, cysteine-rich secretory protein; SVMP INH, snake venom metalloproteinase inhibitor; NGF, nerve growth factor; PLB, phospholipase B; AChE, acetylcholinesterase.

* Corresponding author.
E-mail address: tara.pukala@adelaide.edu.au (T.L. Pukala).

https://doi.org/10.1016/j.bbapap.2023.140992
Received 27 September 2023; Received in revised form 20 December 2023; Accepted 25 December 2023
Available online 27 December 2023

antivenom administration [8].

The urgent need for better antivenom treatments has thus led to the exploration of alternative strategies such as the use of peptide inhibitors and small molecule-based antivenom therapies to target and neutralise specific lethal components in the venom [11–14]. While promising, this targeted strategy requires thorough structural and functional understanding of the venom composition which poses a tremendous challenge due to the highly variable and heterogeneous nature of snake venom. Inter- and intraspecies venom variation, geographical, ontogenic and dietary factors can drastically affect the composition of the venom [15,16]. Furthermore, various toxin proteoforms, where protein sequences differ by a few amino acid residues or by additional structural moieties in the form of post-translational modifications (PTMs), contribute towards the subtle diversity in venom compositions and are increasingly speculated to be important in venom toxicity [17,18].

The advent of 'omics' technology in recent years has enabled significant development of high-throughput strategies to identify and characterise venom proteomes. Bottom-up (BU) proteomic approaches have become well-established pipelines to catalogue venom proteomes where whole venom or venom fractions separated by a chromatographic technique, typically reverse-phase liquid chromatography, are enzymatically digested into smaller peptides for analysis by tandem mass spectrometry (MS/MS) [19,20]. Venom protein identification is then determined by searching the spectral data against a protein database for snake venoms [19,20]. While there is well-established precedence for this type of workflow, this digestion process leads to a disconnect between the original protein and the generated peptides, resulting in the loss of the molecular mass of the intact protein which is valuable in inferring structural variations such as post-translational modifications (PTMs) that contribute towards venom proteoform diversity [21]. Therefore, BU proteomics alone is unable to capture the subtle variations in venom proteoforms that lend diversity to toxins, and orthogonal approaches are needed to supplement BU proteomics.

Intact mass spectrometry has emerged as a complementary technique as it is able to directly measure intact mass of the whole protein which is critical in distinguishing proteoforms and maintaining any PTMs present [22,23]. The application of intact MS in tandem with BU proteomics for characterising venoms is gaining momentum as a way to explore venom diversity from a myriad of snakes, specifically for smaller toxins (<30 kDa), which are more amenable to intact MS analysis [24–31].

In addition, heterogeneity of venom proteins at a higher-order structural level, such as non-covalent interactions that may be important for venom activity, remain poorly characterised. Biophysical strategies such as native MS and mass photometry (MP) are promising yet underexplored approaches that could be used to probe and capture venom protein diversity at the quaternary structural level [32]. Native MS allows direct infusion of the venom samples into the mass spectrometer under gentle ionisation conditions using physiological buffers to maintain proteins in a native-like structural state, and enables rapid detection of protein mass and higher oligomeric species in the gas-phase [33,34]. Mass photometry (MP) as an intrinsically quantitative technique operates on the principle that light scattering of an individual biomolecule in solution is directly proportional of the mass of the biomolecule [35,36]. Given this, the combination of native MS and MP can provide insight into the structural heterogeneity of a venom sample when the protein population is diverse, and importantly, probe for larger non-covalent protein interactions that are not well-preserved by other techniques [35].

In this study, we endeavour to contribute to this growing field and describe the characterisation of the venom from the forest cobra (*Naja melanoleuca*) using an integrated multi-faceted approach. *N. melanoleuca* is the largest species of the true African cobras and is found to inhabit an extensive range of habitats across Western, Southern and Central Africa [37,38]. Despite the snake's propensity to deliver enormous venom yields and the severe envenomation symptoms of systemic paralysis leading to death, the venom of *N. melanoleuca* remains largely underexplored [37].

Endeavours to catalogue the venom composition of *N. melanoleuca* have commenced, using a BU proteomic approach and generic *Serpentes* protein database-searching to identify the venom proteins present [37,39]. Here, we report a venom gland transcriptome-guided BU proteomic analysis of *N. melanoleuca* venom for the first time. Furthermore, we endeavour to explore the *N. melanoleuca* venom heterogeneity using intact MS as well as interrogate selected higher-order protein assemblies using native MS and MP. This work hopes to facilitate characterisation of *N. melanoleuca* venom proteoforms and higher-order structures in order to appreciate venom complexity and diversity, thus furthering our current understanding of the structural and functional roles of venom proteins to subsequently aid more informed antivenom therapies.

2. Materials and methods

2.1. Materials

All reagents were purchased from Sigma Aldrich unless specified otherwise.

Whole lyophilised *N. melanoleuca* venom (pooled from three individual snakes) was purchased from Venom Supplies Pty. Ltd. (Tanunda, Australia) and was stored at −20 °C until required. Venom glands from a *N. melanoleuca* snake were gifted from Venom Supplies Pty. Ltd. (Tanunda, Australia) and were stored in RNAlater solution (Thermo Fisher Scientific) at −20 °C until required.

2.2. Venom gland RNA extraction, sequencing, and bioinformatics

Total RNA was extracted from venom glands of a *N. melanoleuca* snake. Venom gland tissue (25 mg) was excised and homogenised on ice using a microfuge pestle sterilised by RNAse Away reagent (Thermo Fisher Scientific). Total RNA was extracted using the TRIzol reagent method (Thermo Fisher Scientific) prior to purification using the PureLink RNA mini kit (Thermo Fisher Scientific) as per the manufacturer's protocol. Purified RNA was reconstituted in RNAse-free water (80 μL) and RNA QC was performed on a Bioanalyser instrument (Agilent Technologies) with a RNA Integrity Number (RIN) score of 7.4. The sample was stored at −80 °C until required for downstream RNA sequencing analysis.

2.3. RNA sequencing analysis, bioinformatics, and toxin annotation

Total RNA was converted to strand-specific Illumina compatible sequencing libraries using the Nugen Universal Plus Total RNA-Seq library kit from Tecan (Mannedorf) as per the manufacturer's instructions (MO1485 v4), using 12 cycles of PCR amplification for the final libraries. Sequencing of the library pool (2 × 150 bp paired-end reads) was performed on an Illumina Nextseq 500 using a mid-output kit. Raw RNA-seq data of *N. melanoleuca* was first filtered for low quality reads and adapters were removed using TrimGalore (v0.6.7) with default settings [40]. The processed reads were used to perform *de novo* transcriptome assembly using Trinity (v2.8.5). The assembled contigs were then used to perform open reading frame (ORF) prediction from the top strand using TransDecoder (v5.5.0) [41]. Peptides between the lengths 40 to 2730 amino acids were retained for further downstream analysis as this was the range expected for toxin proteins.

Protein sequences were searched against all *Serpentes* protein sequences obtained from the UniProt protein database (database downloaded on 12th November 2022) using command line BLAST (v2.13.0) with default settings [42]. Only the top BLAST hit for each sequence was retained for further filtering based on an e-value $<10^{-4}$. The filtered peptide sequences were then further distinguished into non-toxins and toxins, with the latter group annotated and further categorised into respective toxin families.

2.4. Chromatographic fractionation of whole venom

Venom proteins were fractionated by size exclusion chromatography (SEC). Lyophilised *N. melanoleuca* venom was reconstituted in 200 mM ammonium acetate (NH_4OAc, pH 6.8) at a concentration of 10 mg/mL and loaded onto a Superdex200 10/300 size exclusion column (GE Healthcare), coupled to an ÄKTA Pure FPLC system (GE Healthcare). Prior to sample loading (600 μL), the column was equilibrated with 200 mM NH_4OAc (pH 6.8) as the eluent. Fractions (400 μL) were collected at a flowrate of 0.4 mL/min over a volume of 36 mL using an isocratic gradient. Venom fractions were visualised by gel electrophoresis; fractions containing protein species of similar molecular mass based on the gel analysis were pooled and concentrated to a final volume of 50 μL using Amicon Ultra-0.5 mL centrifugal filter units (Merck Millipore) with a 3 kDa molecular mass cut-off. Total protein concentrations of each of the pooled venom fractions were determined using a colorimetric Pearce™ bicinchoninic acid (BCA) protein assay (Thermo Fisher Scientific) as per the manufacturer's protocol. Samples were stored at −20 °C until required for further analysis.

2.5. 1D SDS-polyacrylamide gel electrophoresis

Pooled venom fractions of interest were added in a 1:1 (*v/v*) ratio to 5× non-reducing sample buffer (150 mM Tris-HCl, 6% SDS, 30% glycerol, 0.3% bromophenol blue, pH 6.8). The same fractions were also added in a 1:1 (*v/v*) ratio to 5× reducing sample buffer (300 mM DTT, non-reducing sample buffer recipe). Both sets of samples were denatured at 95 °C for 20 min prior to loading on to a 4–15% Mini-Protean TGX Tris-HCl polyacrylamide gel (Bio-Rad Laboratories). Gel electrophoresis was performed at 140 V and 400 mA for 50 min in 1 x SDS tris-glycine running buffer. Novex Sharp unstained protein standards (Thermo Fisher Scientific) were used as protein molecular mass markers. SDS-PAGE gels were then visualised by Coomassie Brilliant Blue staining (Coomassie Brilliant Blue R250 dye, 40% (*v/v*) methanol, 10% (*v/v*) glacial acetic acid) prior to imaging using a ChemiDoc XRS+ imaging system (Bio-Rad Laboratories).

2.6. In-solution tryptic digestion

Venom SEC samples (50 μg total protein) were treated with 50 mM dithiothreitol (DTT) in 7 M urea/100 mM ammonium bicarbonate (100 μL), and incubated at 37 °C for 1 h. The samples were further incubated with 55 mM iodoacetamide (IAA) in 7 M urea/100 mM ammonium bicarbonate (100 μL) for 20 min in darkness. The samples were diluted with 50 mM ammonium bicarbonate (400 μL) and Promega MS grade trypsin (Thermo Fisher Scientific), resuspended at 0.1 μg/μL in 10 mM ammonium bicarbonate, was added to the venom samples at a mass ratio of 1:50 (trypsin:protein). The venom samples were incubated at 37 °C overnight before being quenched with trifluoroacetic acid (TFA) at a final concentration of 1%. The digested peptides were dried by vacuum centrifugation and reconstituted in 2% acetonitrile (ACN)/ 0.1% formic acid (FA) (*v/v*) (50 μL). The peptides were then purified using C_{18} Biospin columns (Thermo Fisher Scientific), and sample concentrations were determined using a NanoDrop 2000/2000c UV–Vis spectrophotometer at a wavelength of 205 nm and an extinction coefficient ε_{205} of 31 $mL.mg^{-1}.cm^{-1}$ [43]. Samples were stored at −20 °C until required for further LC-MS/MS analysis.

2.7. LC-MS/MS analysis of venom fractions

Digested venom samples were analysed using an Ultimate 3000 nano-LC system (Thermo Fisher Scientific) coupled to a LTQ XL Orbitrap mass spectrometer (Thermo Fisher Scientific). Peptide sample (1.5 μg) was pre-concentrated on a C_{18} trapping column (Acclaim PepMap 100 C_{18} 75 μm × 20 mm, Thermo Fisher Scientific) at a flowrate of 5 μL/min using 2% ACN/0.1% TFA (*v/v*) over 10 min. Peptides were then separated using a C_{18} analytical nano-column (Acclaim PepMap100 C_{18} 75 μm × 50 cm, Thermo Fisher Scientific) at a flowrate of 0.3 μL/min. A linear gradient of 5% to 45% of solvent B was applied over 38 min. This was followed by a 2 min wash with 90% B, then a 15 min equilibration process with 5% B. (Solvent A: 2% ACN/ 0.1% FA (*v/v*). Solvent B: 80% ACN/ 0.1% FA (*v/v*)). LC-MS/MS acquisitions were controlled by Xcalibur v2.1 (Thermo Fisher Scientific) and the mass spectrometer was operated in data-dependent acquisition mode. Spectra were acquired in positive polarity over the mass range of 300–2000 *m/z* at a resolution of 60, 000 in FT mode. The 5 most intense precursor ions were further selected for CID fragmentation using a dynamic exclusion of 5 s where the dynamic exclusion criteria included a minimum relative signal intensity of 1000 and ≥ 2+ charge state. An isolation width of 3.0 *m/z* and a normalised collision energy of 35 were used. The mass spectrometry proteomics data have been deposited to the ProteomeXchange Consortium *via* the PRIDE partner repository with the dataset identifier PXD045209 and https://doi.org/10.6019/PXD045209.

Raw MS/MS data was submitted for qualitative protein identification using Proteome Discoverer (v2.5, Thermo Fisher Scientific). The data was searched against all entries in the custom *N. melanoleuca* venom gland transcriptome database using Sequest HT as the search engine. Search parameters were as follows: tryptic peptides with a maximum of 2 missed cleavages were allowed, peptide mass tolerance of 20 ppm, fragment mass tolerance of 0.8 Da, cysteine carbamidomethylation set as a static modification and acetylation of the protein N-terminus, methionine oxidation and deamidation of glutamine and asparagine set as dynamic modifications. False positives were identified using a False Discovery Rate (FDR) of 0.05%. False positives, contaminants and any proteins that did not contain a toxic function were eliminated from further analysis. A minimum of 2 unique peptides was set as the threshold for protein identification. The relative semi-quantitative values for a given toxin family were calculated from the sum of the peptide spectrum matches (PSM) generated by Proteome Discoverer.

2.8. LC-MS analysis of intact venom samples

Venom samples were reconstituted in 5% acetonitrile, 0.1% formic acid. Venom samples were analysed using an I-Class Acquity UPLC system coupled to a Xevo G2-XS Q-ToF mass spectrometer (Waters Corporation). Sample (2 μg) was loaded onto an Acquity UPLC Protein BEH C_4 (300 Å pore size, 1.7 μm particle size, 2.1 mm ID x 50 mm bed length) column (Waters Corporation) at a flowrate of 0.3 mL/min. The gradient for Solvent B used was as follows: 5% to 15% over 1 min, 15% to 55% over 8 min, 55% to 95% over 1 min, held at 95% over 1 min, 95% to 5% over 1 min and held at 5% for 2 min (Solvent A: 99.9% MS-grade water/ 0.1% FA (*v/v*). Solvent B: 99.9% ACN/ 0.1% FA (*v/v*)). Column temperature was maintained at 80 °C. The mass spectrometer instrument conditions were set as follows: *m/z* range, 250–5000; polarity, positive; analyser mode, sensitivity; capillary voltage, 3.5 kV; sampling cone voltage, 80 V; source temperature, 120 °C; desolvation temperature, 300 °C; desolvation gas flow, 800 L/h; source offset, 90; quadrupole profile, 500, 1000, 1500.

2.9. Native MS analysis of larger venom fractions

All native MS experiments were performed on a Bruker Impact II HDMS quadrupole time-of-flight mass spectrometer (Bruker). Venom samples (NM1–3) were buffer-exchanged into 200 mM ammonium acetate buffer prior to analysis. Sample (4 μL) was directly infused into the instrument by nanoESI using platinum-coated borosilicate capillaries prepared in-house. The instrument conditions were set as follows: *m/z* range, 500–8000; polarity, positive; capillary voltage, 2 kV; end plate offset, 500 V; source temperature, 60 °C. All mass spectra were analysed using Bruker Compass Data Analysis software (Bruker), and smoothed across 0.5 Da per 2 cycles.

2.10. Mass photometry analysis of larger venom fractions

Venom samples (NM1–3) were diluted with 0.22 μm filtered 200 mM ammonium acetate. Mass calibrations were performed using bovine serum albumin and thyroglobulin as standard proteins. Venom samples were diluted to a final total protein concentration of approximately 34 pg/ μL in 200 mM ammonium acetate and MP experiments were performed on a Two^{MP} instrument (Refeyn Ltd) at room temperature. Objective lens focusing was performed using 200 mM ammonium acetate (10 μL) before venom sample (10 μL) was applied to the same sample well and mixed by rapid pipetting before data acquisition using the software AcquireMP (Refeyn Ltd). The generated video data was processed and analysed using the software DiscoverMP (Refeyn Ltd) where raw interferometric contrast values were converted to molecular mass by applying the standard mass calibration.

3. Results and discussion

3.1. Venom gland transcriptomics

As the venom gland transcriptome affords a global representation of the toxin genes being expressed, it becomes a powerful database to guide downstream proteomic analysis for a more species-specific venom characterisation. In this work, venom gland transcriptomic analysis was first performed on a pair of *N. melanoleuca* venom glands where total RNA was extracted from *N. melanoleuca* venom glands, sequenced and translated into amino acid sequences. Proteins were searched against all known venom toxins in the existing UniProt protein database (*Serpentes* taxonomy), and only protein sequences with a toxin function were retained and further assigned to a toxin family. The number of identified toxin sequences that corresponded to the same family, for instance the 3-finger toxin (3FTx) superfamily, were then filtered for redundancies, summed, and used to construct a view of venom diversity (Fig. 1).

Of 155,769 sequences, 1619 possessed a toxin function and contributed towards the generated toxin transcriptome database (Fig. 1). The high proportion of non-toxins is not unexpected as they most likely corresponded to housekeeping and regulatory proteins within the venom glands.

The venom gland transcriptome of *N. melanoleuca* appeared to be diverse with 22 distinct toxin superfamilies identified. Three-finger toxin (3FTx, 15.4%) was shown to be the most abundant toxin family, followed by the snake venom metalloproteinase and disintegrin superfamily (SVMP-DIS, 12.8%), snake venom serine protease (SVSP, 12.2%), phosphodiesterase (PDE, 10.3%), and C-type lectin (CTL, 10.3%) families. The two other major toxin groups phospholipase A_2 (PLA_2, 5.4%) and L-amino acid oxidase (LAAO, 5.1%) were also accounted for, and minor toxin families including cystatin (CYS, 3.6%), 5'nucleotidase (5'NUC, 3.1%), cobra venom factor (CVF, 2.5%), aminopeptidase (AP, 1.2%), snake venom serine protease inhibitor (SVSP INH, 1.0%), hyaluronidase (HYAL, 0.7%), hydrolase (HYD, 0.7%), phospholipase A_2 inhibitor (PLA_2 INH, 0.6%), cysteine-rich secretory protein (CRiSP, 0.6%), snake venom metalloproteinase inhibitor (SVMP INH, 0.4%), nerve growth factor (NGF, 0.4%), phospholipase B (PLB, 0.3%), and acetylcholinesterase (AChE, 0.1%) constituted the rest of the transcriptome. To our knowledge, here we report the venom gland transcriptome for *N. melanoleuca* for the first time, and the abundant expression of 3FTx genes observed is a good first indication towards the dominant clinical symptom of neurotoxicity observed in *N. melanoleuca* envenomation, considered largely to be driven by 3FTx proteins [37]. Of note, the venom gland tissues were from the offspring of one of the specimens milked for its venom. We acknowledge this limitation and do not aim to explore in-depth correlation of toxin expression levels between the transcriptome and proteome. Rather, given the exploratory nature of this work, the venom gland transcriptome in Fig. 1 will serve as a custom, species-specific database for downstream protein identification in *N. melanoleuca* venom.

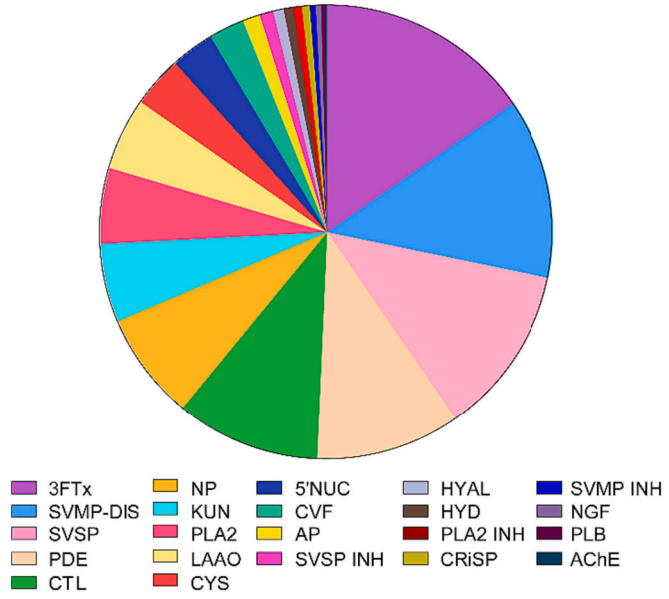

Fig. 1. Toxin gene expression in the venom gland transcriptome of *N. melanoleuca,* where the coloured proportions are a count of different toxin transcripts identified. The 1619 toxin sequences were categorised into 22 toxin families, assigned in descending order from left to right with the number of identified transcripts included: three finger toxin (3FTx, 249), snake venom metalloproteinase and disintegrin (SVMP-DIS, 208), snake venom serine protease (SVSP, 197), phosphodiesterase (PDE, 167), C-type lectin (CTL, 166), natriuretic peptide (NP, 124), kunitz-type serine protease inhibitor (KUN, 90), phospholipase A_2 (PLA_2, 87), L-amino acid oxidase (LAAO, 83), cystatin (CYS, 59), 5'nucleotidase (5'NUC, 50), cobra venom factor (CVF, 41), aminopeptidase (AP, 20), snake venom serine protease inhibitor (SVSP INH, 16), hyaluronidase (HYAL, 12), hydrolase (HYD, 11), phospholipase A_2 inhibitor (PLA_2 INH, 10), cysteine-rich secretory protein (CRiSP, 9), snake venom metalloproteinase inhibitor (SVMP INH, 7), nerve growth factor (NGF, 6), phospholipase B (PLB, 5), and acetylcholinesterase (AChE, 2). Of note, SVMP and DIS are treated as one superfamily here as SVMP and DIS domains are co-expressed at the transcript level [44].

3.2. Fractionation of N. melanoleuca whole venom

In order to begin deconvoluting the complexity of the venom and facilitate increased protein identification, crude whole venom from *N. melanoleuca* was first fractionated by size-exclusion chromatography (SEC) (Fig. 2A). The proteins were eluted in ammonium acetate buffer compatible with downstream MS analysis to maintain any non-covalent protein complexes in a native state. SEC peaks are labelled numerically (NM1–5) along the elution profile for ease of reference, where earlier eluting peaks correspond to larger protein species.

The SEC elution profile for *N. melanoleuca* suggested a complex venom with five main peaks corresponding to various large, intermediate, small protein species with a high abundance of smaller toxins as shown by the relative intensity of SEC peaks NM4 and NM5 (Fig. 2A). Further separation of the protein components in the five peaks of interest was performed using a combination of non-reducing and reducing SDS-PAGE for an additional dimension of molecular mass separation and visualisation. Non-reducing SDS-PAGE analysis reflected the diverse range of protein constituents across the *N. melanoleuca* SEC fractions well (Fig. 2B). Large toxins constituted peak NM1 (60–150 kDa) and peak NM2 (40–150 kDa). Peak NM3 had a range of smaller to intermediate sized proteins (15–50 kDa) whereas small toxins and peptidic species were most abundant in peak NM4 (10–25 kDa) and peak NM5 (<10–25 kDa).

In addition to visualising the protein constituents within the venom fractions, reducing SDS-PAGE enabled rapid screening for potential covalent complexes where shifts in protein bands served as the first

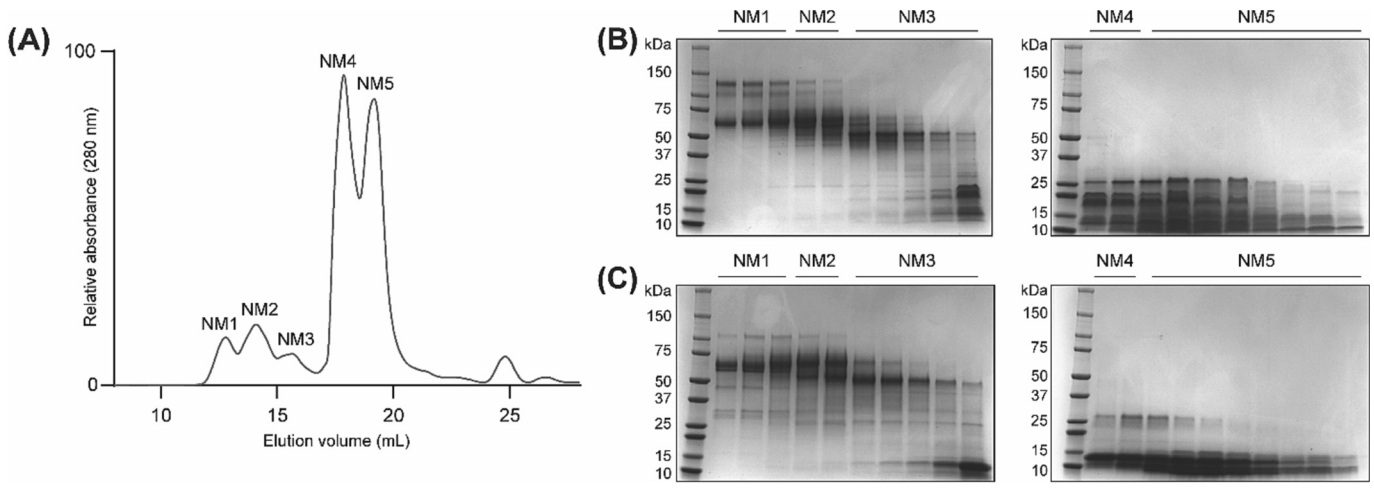

Fig. 2. (A) Size exclusion chromatography (SEC) elution profile of whole venom from *N. melanoleuca*. The eluted fractions across each SEC peak are labelled with the corresponding peak numbers as NM1–5. SEC fractions corresponding to each peak were further visualised using SDS-PAGE analysis under (B) non-reducing and (C) reducing conditions.

indication of the disruption of covalent protein structures (Fig. 2C). Notably for fractions corresponding to peak NM1, protein bands of approximately 30 kDa, 50 kDa and 70 kDa were observed with the disappearance of the 150 kDa protein band, suggesting that these may be subunits of a larger covalent complex. For peak NM2, the appearance of protein bands corresponding to approximately 25 kDa under reducing conditions also implied the presence of a larger covalent complex within the diverse mixture of proteins. Fractions corresponding to peaks NM3, NM4 and NM5 also showed the disappearance of protein bands at 25 kDa, indicating the presence of smaller covalent complexes in the venom that could be disrupted to monomeric species. Furthermore, SDS-PAGE analysis of the crude venom under non-reducing and reducing conditions showed no variations in protein bands to Fig. 2, confirming that the SEC peaks NM1–5 comprehensively capture the full range of proteins in *N. melanoleuca* venom (supplementary Fig. S1).

3.3. Proteomic composition of *N. melanoleuca* venom fractions

To catalogue the proteomic composition of the *N. melanoleuca* venom, the five SEC venom fractions were enzymatically digested into peptides and analysed by LC-MS/MS using a BU proteomic approach. Identification of the various toxin families present in the venom fractions was performed by searching the proteomic spectra data against the transcriptome-derived database for *N. melanoleuca* venom (Fig. 1); the list of identified proteins is provided in supplementary data, Table S1. The number of peptide spectrum matches (PSMs) for a given protein hit in the search is used here as a simple estimation of relative abundance [45,46]. As venom compositions are extremely prone to both inter and intraspecies variations, absolute quantification of the venom components was not the intention in this study. Here, the identification of toxin families in the venom was of primary interest and the sum of the PSMs for protein hits corresponding to the same toxin family was taken. The toxin families identified in each fraction are shown as different coloured proportions, relative to the sum of the PSMs for a given toxin family in Fig. 3.

As shown in Fig. 3, the collective proteomic composition of the venom fractions revealed a diverse repertoire of six toxin superfamilies: CVF, LAAO, SVMP-DIS, 3FTx, PLA_2 and NP. In this analysis, SVMP and DIS are still referred to as the superfamily SVMP-DIS based on the transcriptome-derived library the proteomic data was searched against.

In the earlier eluting venom fractions NM1 and NM2, larger protein components such as CVF, LAAO and SVMP-DIS were the dominant constituents. Notably, we report a prominent abundance of CVF toxins in this venom compared to previous proteomic studies, which is possibly attributed to intraspecies venom variability [37,39]. Fraction NM3 is the most diverse, with five toxin families: SVMP-DIS, PLA_2, 3FTx, CVF and LAAO, which correlates well with the fact that fraction NM3 is intermediate between the high and low molecular mass venom fractions. The smaller fractions NM4 and NM5 are dominated by low molecular mass toxins belonging to PLA_2 and 3FTx superfamilies. Lower abundant toxins from SVMP-DIS and NP families were also identified in fraction NM4. The abundance of 3FTx in this venom is noteworthy as 3FTx is a

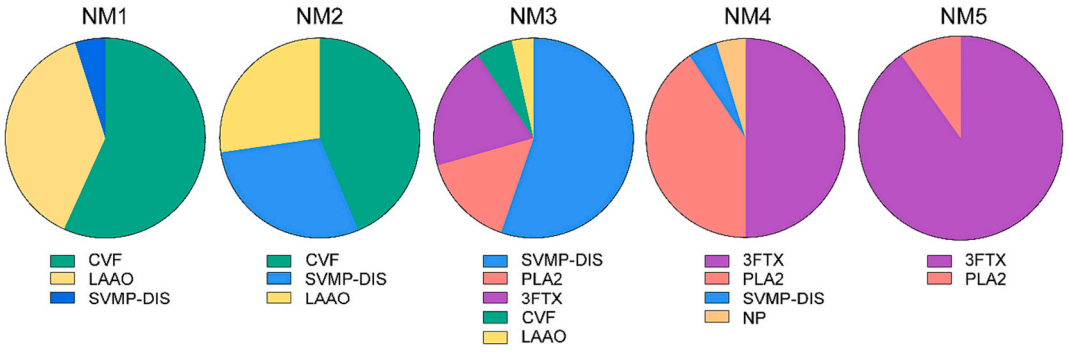

Fig. 3. Proteomic compositions of the five SEC fractions from *N. melanoleuca* venom. Toxin families in each venom fraction were identified by database searching using the transcriptome-derived *N. melanoleuca* toxin database. Each coloured proportion corresponds to a distinct toxin family and the size of the proportion is relative to the sum of the PSMs for a given toxin family.

group of post-synaptic neurotoxins that are known to be potent in driving neurotoxicity and paralysis, which are characteristic symptoms of envenomation by cobra (*Naja*) venom [47]. Furthermore, coagulotoxicity has been reported as an underlying symptom for various cobra envenomation; several cobra species have been shown to produce anticoagulant effects by inhibiting blood coagulation factors, which other toxin families such as PLA_2 and SVMP-DIS may have been strongly facilitating [47]. While this is not well-understood for *N. melanoleuca,* we speculate PLA_2 and SVMP-DIS toxins may be involved in a similar role.

Comparison between the toxin genes detected in *N. melanoleuca* venom glands and the secreted venom protein composition showed a relatively modest correlation between these two levels. While the dominance of 3FTx and SVMP-DIS toxin gene expressions was consistently observed across both toxin gene and protein expression levels, there were other toxin families that were not as abundantly expressed at the protein level, such as SVSP. However, as the lack of SVSP toxins was also noted in previous proteomic studies for this snake venom, this may be intrinsic to *N. melanoleuca* venom and may imply another level of regulation between toxin gene transcription and protein translation for certain toxin families [37,39]. It is well-known that modest correlations between the transcriptomic and the proteomic expression levels occur often in other systems and are common for snake venoms as well [15,48,49].

The dominance of the six toxin families observed at the protein level highlights the significance of these toxins in defining the venom profile of *N. melanoleuca.* Nevertheless, the use of a species-specific venom gland transcriptome-derived database to guide the identification of venom proteins in this work was able to reveal the diverse and 3TFx-rich venom proteome as well as highlight some interesting diversity between the transcription and protein translation levels in *N. melanoleuca* venom for the first time.

3.4. Intact LC-MS analysis of N. melanoleuca venom fractions

While BU proteomics can identify the various toxin families that constitute the venom fractions, the subtle diversity of different proteoforms is not well-captured. In order to explore the proteoform variations within *N. melanoleuca* venom and to afford another dimension of separation, SEC venom fractions were further separated by RP-UPLC and directly coupled to the mass spectrometer for intact MS analysis. The chromatograms of the five SEC venom fractions with LC peaks annotated with the deconvoluted intact protein masses at the corresponding retention time are shown below (Fig. 4). A detailed list of the proteins, corresponding intact masses and retention times can be found in supplementary data, Table S2.

Of note, preliminary top-down proteomic sequencing was attempted for these venom proteins, but owing to the extremely robust nature of these toxins, generation of informative fragment ions for sequence matching proved to be difficult and would require extensive optimisation (supplementary Fig. S2). Thus, this study explored the proteoform profiling at a more general proteoform level based on intact mass measurements, and putative toxin families were tentatively assigned to each identified intact proteoform by inference from experimentally determined masses, known literature molecular masses for specific toxin families, and the corresponding toxin families identified in the BU proteomic analysis for each venom fraction.

LC-MS analysis revealed the subtle diversity in various toxin families across all fractions that was otherwise not evident in the BU proteomics analysis alone. The two highest molecular mass venom fractions NM1 and NM2 contained proteoforms corresponding to the LAAO, SVMP and DIS toxin families (Fig. 4A and B). Notably, we begin to appreciate the various proteoforms of what appears to predominantly belong to SVMP and DIS toxin families. Here, SVMP and DIS have been referred to as separate protein families since there are various sub-types of processed forms of the SVMP-DIS superfamily upon protein maturation, including

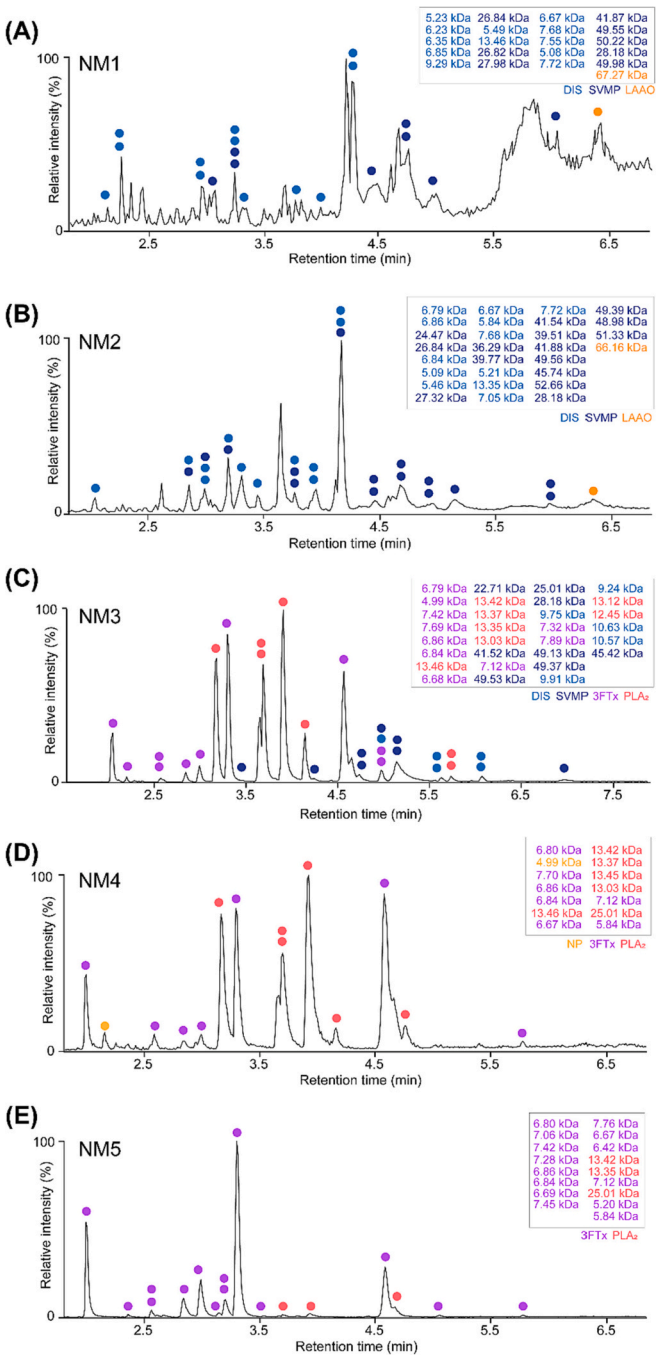

Fig. 4. Denaturing LC-MS analysis of the five SEC fractions of *N. melanoleuca* venom. Venom fractions (A) NM1, (B) NM2, (C) NM3, (D) NM4, and (E) NM5 were separated by RP-UPLC and analysed under denaturing conditions by top-down mass spectrometry. The intact masses of all resolvable proteoforms were determined and the protein species eluting across the various chromatograms are denoted by the coloured circles. The corresponding protein mass for each species is shown in the mass list (inset), assigned in elution order from left to right. The annotated colours correspond to the following toxin families that have been putatively assigned, based on intact mass measurements and reported literature masses for the toxin families: DIS (light blue), SVMP (dark blue), LAAO* (orange), 3FTx (purple), PLA_2 (red), NP* (yellow). Ambiguous toxin family assignments have been denoted with an asterisk. (For interpretation of the references to colour in this figure legend, the reader is referred to the web version of this article.)

the proteolytic release of the DIS domain from the SVMP domain, and the intact mass measurements enable distinctions of these domains for general protein assignment [44]. Of note, the list of proteoforms presented here is not all-encompassing as there were larger protein MS peaks that could not be resolved and mass deconvolved, impeded by what appeared to be complex post translational modifications (PTMs) in addition to intrinsically poorer ionisability of larger proteins (supplementary Fig. S3). Many of these unresolved peaks may well correspond to larger venom proteins belonging to CVF and LAAO toxin families which would account for the lack of these toxin families in the analysis despite being abundant in the BU proteomic results (Fig. 3).

Intact MS analysis for fraction NM3 showed toxin family diversity that is consistent with the BU proteomic results, where SVMP, PLA_2, DIS and 3FTx proteoforms were assigned (Fig. 4C). The lowest molecular mass venom fractions NM4 and NM5 had many proteoforms that corresponded to PLA_2 and 3FTx toxin families, with NP proteoforms tentatively assigned to fraction NM4 (Fig. 4D and E). To our knowledge, the subtle diversity in these venom proteoforms have not been explored or well-reported for *N. melanoleuca* venom. At the time of writing, there are only 15 reviewed venom proteins from *N. melanoleuca* reported in the Uniprot database, all belonging to either PLA_2 or 3FTx families. Of the 15 protein entries, 12 have been identified in our study based on the combination of BU proteomic and LC-MS analyses (supplementary Table S3). While three of the Uniprot entries were not observed here potentially due to slight intraspecies variations, our study is overall in good agreement with literature and reveals additional PLA_2 and 3FTx proteoforms that have not been reported yet. This showcases the significance of using various techniques to catalogue and appreciate the subtle variations in these smaller toxins and their contribution to venom diversity, especially given their high abundance and potential role in the characteristic symptoms of envenomation. Furthermore, small toxins have also been reported to be difficult components to target during antivenom treatment as they have poorer immunogenicity and can evade antivenom neutralisation, further underpinning the importance of characterising these species [8,50,51].

It is noteworthy that inevitable ambiguity in assignment was present for some of the intact masses that could have corresponded to different toxin families overlapping in similar molecular mass ranges. In particular, tentative assignments for toxin families such as LAAO were made. The intact mass of the LAAO species also correlated to SVMPs; these two toxin families are known to have variable post-translational modifications which renders it difficult to confidently assign the mass measurement to a given toxin family. Thus, the putative assignments made were based on the most relatively abundant toxin family observed in the BU proteomics analysis (Fig. 3). To circumvent this ambiguity, future endeavours would encompass a top-down proteomic approach where the intact proteins are further subjected to fragmentation and the fragment ions searched against the targeted venom protein database. Given the fact that intact venom proteins are extremely robust and difficult to fragment (supplementary Fig. S2), sample preparation strategies and optimising fragmentation techniques would be the first necessary steps towards achieving comprehensive proteoform sequencing. The rigour of proteoform assignment by top-down proteomics is beyond the scope of this study; nonetheless, the LC-MS analysis here reveals the extent of venom heterogeneity and serves as a foundation for future top-down proteomic endeavours.

3.5. *Higher-order structural interrogation of larger venom fractions*

Since some of the larger venom proteins were not as amenable to the denatured LC-MS workflow as the smaller toxins, a novel combination of two biophysical techniques, native MS and mass photometry (MP), was used to interrogate the venom fractions NM1–3 and probe for higher-order protein interactions (Fig. 5).

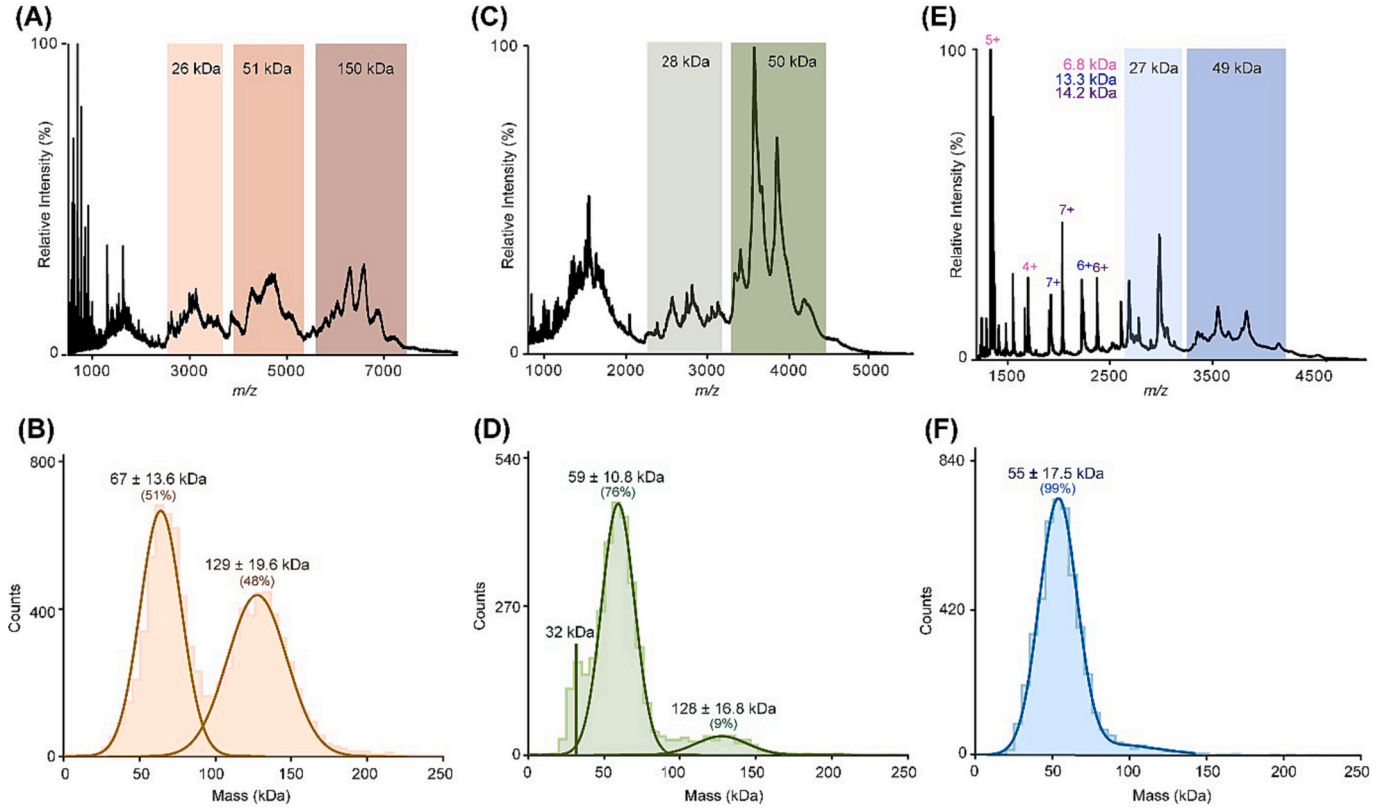

Fig. 5. Higher-order structural characterisation of large venom fractions from *N. melanoleuca*. Native MS analysis of SEC fractions (A) NM1, (C) NM2, and (E) NM3 were acquired in 200 mM ammonium acetate (pH 6.8). Mass photometry analysis was performed on fractions (B) NM1, (D) NM2, and (F) NM3 in the same buffer conditions as the native MS analysis with single-particle counts plotted as histograms and fitted to Gaussian distributions.

From Fig. 5, the heterogeneity of these venom samples is reflected in the native MS analysis where multiple proteoforms exist within the various mass distributions. Each mass distribution was approximated considering the significant peak broadening in fractions NM1–3 rendered it difficult to perform accurate mass deconvolution for many of the protein species (Fig. 5A, C, E). However, these broad peaks are also strong indication of post-translational modifications (PTMs) [52]. The presence of extensive glycosylation in these venom proteins was confirmed by the deglycosylation treatment to remove *N*-glycans using the enzyme peptide-*N*-glycosidase F (PNGase F). Visualisation of venom fractions NM1–3 by SDS-PAGE showed distinct shifts in various protein bands, indicating the loss of glycan moieties (supplementary Fig. S5). The presence of glycosylation on these larger venom proteins supports the spectral peak broadening observed in the native MS analysis as this effect arises from the intrinsically heterogeneous nature of glycans, further adding to the complexity of protein heterogeneity (Fig. 5). Importantly, glycosylation is known to be a prevalent PTM in larger venom proteins and has been previously observed in toxin families such as CVF, LAAO, SVSP and SVMP in other snake venoms [44,53–55]. Such modifications have been speculated to be important in providing enhanced activity, structural stability and solubility as well as lending steric bulk to protect these larger venom proteins from degradation [56–58]. Given this, the role of glycosylation here may well serve similar protective functions in *N. melanoleuca* venom. Future studies would encompass more in-depth structural interrogation of these highly glycosylated venom proteins from a top-down proteomic approach with a focus on glycan profiling to better understand the structural and functional role of these PTMs.

In terms of the heterogeneity observed in venom fraction NM1, three main mass distributions at approximately 26 kDa, 51 kDa and 150 kDa were noted in the native MS analysis (Fig. 5A). While exact proteoform assignment is difficult without top-down proteomic sequencing, the speculated toxin identities for these larger species were still tentatively inferred based on the BU proteomic analysis for each venom fraction and the molecular mass ranges known to be characteristic for each toxin family in literature. Given this, the 150 kDa distribution may likely encompass a CVF toxin or higher-order structures of LAAO whereas the 26 kDa and 50 kDa populations likely correspond to various SVMP proteoforms and monomeric LAAO species, respectively (Fig. 3). Further MP analysis confirmed the presence of the two higher molecular mass distributions at 67 ± 14 kDa and 129 ± 20 kDa (Fig. 5B). As these are lower resolution analyses, the mass discrepancies between the two techniques were not unreasonable, with most native MS assignments still within the standard deviation ranges from the MP measurements.

For fraction NM2, two distributions at approximately 28 kDa and 50 kDa were determined by native MS whereas MP analysis captured two higher mass distributions – one predominant distribution at 59 ± 11 kDa and a low abundance distribution at 128 ± 17 kDa (Fig. 5C and D). The latter distribution was not observed by native MS, most likely due to poorer intrinsic ionisation. Given the similar venom compositions between fraction NM1 and NM2 based on the BU proteomic analysis (Fig. 3), the species observed at 59 kDa corresponds well to SVMP or LAAO proteoforms, and the 128 kDa distribution may be a CVF or covalent dimers of SVMP and LAAO toxins (Fig. 5C and D).

For fraction NM3, native MS analysis showed a heterogeneous mixture of lower molecular mass proteins that could be mass deconvolved, along with two other protein populations at around 27 kDa and 49 kDa (Fig. 5E). These larger mass distributions may well be SVMP proteoforms given the abundance of this toxin family in the BU proteomic and LC-MS analyses, while the smaller proteins ranging from 6 to 14 kDa correspond well to 3FTx and PLA_2 toxins (Fig. 5E). In the MP analysis, only a single dominant mass distribution at 55 ± 18 kDa was observed.

Of note, while the absence of <30 kDa species in the MP analysis was observed, this was not unexpected as this mass range coincides with the physical lower limit for MP [59]; below this limit, particles are unable to generate a strong interferometric contrast that would produce an accurate mass measurement. Optical fluctuations, known as shot noise, also become significantly pronounced in this low-end mass region, rendering measurements below 30 kDa more unreliable [60]. Even the slight shoulder peak annotated as 32 kDa in fraction NM2 is largely due to shot noise (Fig. 5D). Thus, the absence of smaller toxin species in the MP analysis was not unexpected.

However, this does not invalidate the presence of these lower molecular mass species as they are still observed in the native MS analysis (Fig. 5A,C,E). This is most likely due to enhanced ionisation effects of these smaller species and the relative intensities in the MS analysis are not a quantitative indication. MP as a quantitative, single-particle counting technique still accurately captures the abundance of the higher molecular mass species (Fig. 5), which is in agreement with the previous SDS-PAGE results that showed NM1–3 to be predominantly comprised of >50 kDa species (Fig. 2B). Here, native MS simply identifies species that may be present in the samples and lends a sensitivity to the low mass range species that may not have been well-captured by the SDS-PAGE analysis (Fig. 2B).

In this study, the observed mass distributions reported above in these higher molecular mass venom fractions appeared to correlate to either monomeric species or covalent higher-order structures. Non-covalent complexes were not observed as treating the venom fractions under denaturing MS conditions that would otherwise disrupt any weakly-held interactions, did not result in any drastic shifts indicative of protein subunit dissociation (supplementary Fig. S4). Higher mass distributions corresponding to non-covalent protein interactions were also not observed in the MP analysis (Fig. 5B,D,F). Although these interactions were not identified in this study, it is important to recognise the complementary potential of native MS and MP and how it lends itself to validating traditional techniques such as SDS-PAGE. MP was able to capture a larger 128 kDa species that was not observed in native MS, likely due to the low abundance nature of this species in the presence of highly ionisable species in the mixture. In contrast, native MS remains ideal for capturing the smaller protein species that are below the lower mass range limit for MP. Taken together, we demonstrate a promising proof of principle and envisage native MS and MP becoming a powerful set of techniques to rapidly probe for interesting non-covalent interactions in other venom systems.

4. Conclusions

Here we have characterised the venom of *N. melanoleuca* using an integrated workflow and demonstrated the use of a multi-faceted approach to begin interrogating the heterogeneity of snake venom. Transcriptomic analysis of the *N. melanoleuca* venom glands showed the diverse expression of toxin genes, encompassing 22 toxin superfamilies. We have generated a transcriptome-derived toxin database to guide downstream proteomic findings for the first time for *N. melanoleuca,* where BU proteomics revealed a diverse and 3FTx-rich venom proteome.

Further separation by RP-UPLC coupled to intact MS analysis allowed for broad profiling of the venom fractions and revealed a diverse repertoire of proteoforms in various toxin families, specifically in the smaller 3FTx and PLA_2 toxins. The subtle diversity suggests small PTMs along with possible amino acid variations, however the exact sequences and finer structural details remain to be explored. A top-down proteomic approach to ascertain exact sequences would be the next important step towards better characterising these proteoforms and understanding their roles in toxicity and in aiding the development of effective targeted therapeutic agents to neutralise these toxic components.

Importantly, we demonstrated the novel use of native MS and MP to explore the heterogeneity of the higher molecular mass venom fractions that were not as amenable to intact MS analysis as the smaller toxins. Notably, variations of 26 kDa, 50 kDa and 150 kDa protein species constituted these venom fractions and have been putatively assigned as

SVMP, LAAO and CVF toxin proteoforms. The complexity of these proteins was further shown to be largely due to extensive glycosylation modifications on these proteins. Future studies would encompass glycoproteomic characterisation of these species to better understand how these modifications contribute to the structure and function of the venom proteins.

The highly heterogeneous nature of snake venoms is multi-faceted, encompassed by intrinsic inter- and intra-species variability, diversity in proteoforms and a multitude of PTMs. While ongoing effort to develop robust and high-throughput venom screening pipelines is required, this study nonetheless presents an overarching profile of *N. melanoleuca* venom, utilising an approach that combines omics with intact MS and other biophysical techniques, and establishes a foundation on which further characterisation studies can be built upon or applied to the investigation of other snake venoms.

CRediT authorship contribution statement

C. Ruth Wang: Writing – review & editing, Writing – original draft, Methodology, Investigation, Formal analysis, Data curation, Conceptualization. **Alix C. Harlington:** Writing – review & editing, Project administration, Formal analysis, Data curation. **Marten F. Snel:** Writing – review & editing, Supervision, Methodology, Formal analysis, Data curation. **Tara L. Pukala:** Writing – review & editing, Supervision, Resources, Project administration, Methodology, Investigation, Funding acquisition, Formal analysis, Conceptualization.

Declaration of Competing Interest

Chia-De Ruth Wang reports financial support was provided by Australian Government. Alix Harlington reports financial support was provided by Australian Government.

Data availability

Data will be made available on request.

Acknowledgements

The authors acknowledge the University of Adelaide Biochemistry Trust Fund for financial support. CRW and ACH were supported by Australian Government Research Training Program Scholarships from the University of Adelaide. We thank the South Australian Genomics Centre (SAGC) for their assistance with RNA-sequencing and both SAGC and the Australian Genome Research Facility (AGRF) for their involvement in the bioinformatics of the transcriptomic analysis. We also thank Venom Supplies Pty. Ltd. for gifting us the *N. melanoleuca* venom glands and Adelaide Microscopy for access to a mass photometer.

Appendix A. Supplementary data

Supplementary data to this article can be found online at https://doi.org/10.1016/j.bbapap.2023.140992.

References

[1] J.M. Gutierrez, J.J. Calvete, A.G. Habib, R.A. Harrison, D.J. Williams, D.A. Warrell, Snakebite envenoming, Nat. Rev. Dis. Primers. 3 (2017) 1–21.
[2] J.P. Chippaux, Snake-bites: appraisal of the global situation, Bull. World Health Organ. 75 (1998) 515–524.
[3] A. Kasturiratne, A.R. Wickremasinghe, N. de Silva, N.K. Gunawardena, A. Pathmeswaran, R. Premaratna, L. Savioli, D.G. Lalloo, H.J. de Silva, The global burden of snakebite: a literature analysis and modelling based on regional estimates of envenoming and deaths, PLoS Med. 5 (2008) 1591–1604.
[4] R. Doley, R.M. Kini, Protein complexes in snake venom, Cell. Mol. Life Sci. 66 (2009) 2851–2871.
[5] Y.S. Chan, R.C.F. Cheung, L. Xia, J.H. Wong, T.B. Ng, W.Y. Chan, Snake venom toxins: toxicity and medicinal applications, Appl. Microbiol. Biotechnol. 100 (2016) 6165–6181.
[6] S. Xiong, C. Huang, Synergistic strategies of predominant toxins in snake venoms, Toxicol. Lett. 287 (2018) 142–154.
[7] T.S. Kang, D. Georgieva, N. Genov, M.T. Murakami, M. Sinha, R.P. Kumar, P. Kaur, S. Kumar, S. Dey, S. Sharma, A. Vrielink, C. Betzel, S. Takeda, R.K. Arni, T.P. Singh, R.M. Kini, Enzymatic toxins from snake venom: structural characterization and mechanism of catalysis, FEBS J. 278 (2011) 4544–4576.
[8] A. Alangode, K. Rajan, B.G. Nair, Snake antivenom: challenges and alternate approaches, Biochem. Pharmacol. 181 (2020) 1–8.
[9] S.A. Seifert, J.O. Armitage, E.E. Sanchez, Snake envenomation, N. Engl. J. Med. 386 (2022) 68–78.
[10] D.G. Lalloo, R.D. Theakston, Snake antivenoms, J. Toxicol. Clin. Toxicol. 41 (2003) 277–290.
[11] M.R. Lewin, L.L. Gilliam, J. Gilliam, S.P. Samuel, T.C. Bulfone, P.E. Bickler, J. M. Gutierrez, Delayed LY333013 (Oral) and LY315920 (intravenous) reverse severe neurotoxicity and rescue juvenile pigs from lethal doses of Micrurus fulvius (eastern coral Snake) venom, Toxins (Basel) 10 (2018) 1–17.
[12] M. Lewin, S. Samuel, J. Merkel, P. Bickler, Varespladib (LY315920) appears to be a potent, broad-spectrum, inhibitor of snake venom phospholipase A2 and a possible pre-referral treatment for envenomation, Toxins (Basel) 8 (2016) 1–16.
[13] W. Bryan-Quiros, J. Fernandez, J.M. Gutierrez, M.R. Lewin, B. Lomonte, Neutralizing properties of LY315920 toward snake venom group I and II myotoxic phospholipases A2, Toxicon 157 (2019) 1–7.
[14] P.G. Gutierres, D.R. Pereira, N.L. Vieira, L.F. Arantes, N.J. Silva Jr., K.A. Torres-Bonilla, S. Hyslop, K. Morais-Zani, R.M.B. Nogueira, E.G. Rowan, R.S. Floriano, Action of Varespladib (LY-315920), a phospholipase a(2) inhibitor, on the enzymatic, coagulant and haemorrhagic activities of Lachesis muta rhombeata (south-American bushmaster) venom, Front. Pharmacol. 12 (2022) 1–9.
[15] N.R. Casewell, S.C. Wagstaff, W. Wuster, D.A. Cook, F.M. Bolton, S.I. King, D. Pla, L. Sanz, J.J. Calvete, R.A. Harrison, Medically important differences in snake venom composition are dictated by distinct postgenomic mechanisms, Proc. Natl. Acad. Sci. U. S. A. 111 (2014) 9205–9210.
[16] J.P. Chippaux, V. Williams, J. White, Venom variability methods of study, results and interpretations, Toxicon 29 (1991) 1279–1303.
[17] D. Andrade-Silva, D. Ashline, T. Tran, A.S. Lopes, S.R. Travaglia Cardoso, M.D. S. Reis, A. Zelanis, S.M.T. Serrano, V. Reinhold, Structures of N-Glycans of Bothrops venoms revealed as molecular signatures that contribute to venom phenotype in viperid snakes, Mol. Cell. Proteomics 17 (2018) 1261–1284.
[18] D. Andrade-Silva, A. Zelanis, E.S. Kitano, I.L. Junqueira-de-Azevedo, M.S. Reis, A. S. Lopes, S.M. Serrano, Proteomic and glycoproteomic profilings reveal that post-translational modifications of toxins contribute to venom phenotype in snakes, J. Proteome Res. 15 (2016) 2658–2675.
[19] B.C. Offor, B. Muller, L.A. Piater, A review of the proteomic profiling of African viperidae and elapidae snake venoms and their antivenom neutralisation, Toxins (Basel) 14 (2022) 1–21.
[20] C.H. Tan, Snake venomics: fundamentals, recent updates, and a look to the next decade, Toxins (Basel) 14 (2022) 1–38.
[21] A.I. Nesvizhskii, R. Aebersold, Interpretation of shotgun proteomic data: the protein inference problem, Mol. Cell. Proteomics 4 (2005) 1419–1440.
[22] K.A. Brown, J.A. Melby, D.S. Roberts, Y. Ge, Top-down proteomics: challenges, innovations, and applications in basic and clinical research, Expert Rev. Proteomics 17 (2020) 719–733.
[23] F. Lermyte, Y.O. Tsybin, P.B. O'Connor, J.A. Loo, Top or middle? Up or down? Toward a standard lexicon for protein top-down and allied mass spectrometry approaches, J Am Soc Mass Spectrom 30 (2019) 1149–1157.
[24] R.D. Melani, O.S. Skinner, L. Fornelli, G.B. Domont, P.D. Compton, N.L. Kelleher, Mapping proteoforms and protein complexes from king cobra venom using both denaturing and native top-down proteomics, Mol. Cell. Proteomics 15 (2016) 2423–2434.
[25] R.D. Melani, F.C.S. Nogueira, G.B. Domont, It is time for top-down venomics, J Venom Anim Toxins Incl Trop Dis 23 (2017) 1–8.
[26] B. Gocmen, P. Heiss, D. Petras, A. Nalbantsoy, R.D. Sussmuth, Mass spectrometry guided venom profiling and bioactivity screening of the Anatolian meadow viper, Vipera anatolica, Toxicon 107 (2015) 163–174.
[27] D. Petras, P. Heiss, R.A. Harrison, R.D. Süssmuth, J.J. Calvete, Top-down venomics of the east African green mamba, Dendroaspis angusticeps, and the black mamba, Dendroaspis polylepis, highlight the complexity of their toxin arsenals, J. Proteomics 146 (2016) 148–164.
[28] D. Petras, P. Heiss, R.D. Sussmuth, J.J. Calvete, Venom proteomics of Indonesian king cobra, Ophiophagus hannah: integrating top-down and bottom-up approaches, J. Proteome Res. 14 (2015) 2539–2556.
[29] D. Petras, B.F. Hempel, B. Gocmen, M. Karis, G. Whiteley, S.C. Wagstaff, P. Heiss, N.R. Casewell, A. Nalbantsoy, R.D. Sussmuth, Intact protein mass spectrometry reveals intraspecies variations in venom composition of a local population of Vipera kaznakovi in northeastern Turkey, J. Proteomics 199 (2019) 31–50.
[30] D. Pla, D. Petras, A.J. Saviola, C.M. Modahl, L. Sanz, A. Perez, E. Juarez, S. Frietze, P.C. Dorrestein, S.P. Mackessy, J.J. Calvete, Transcriptomics-guided bottom-up and top-down venomics of neonate and adult specimens of the arboreal rear-fanged Brown Treesnake, Boiga irregularis, from Guam, J. Proteomics 174 (2018) 71–84.
[31] P. Ghezellou, V. Garikapati, S.M. Kazemi, K. Strupat, A. Ghassempour, B. Spengler, A perspective view of top-down proteomics in snake venom research, Rapid Commun. Mass Spectrom. 33 (Suppl. 1) (2019) 20–27.
[32] L.E. Kilpatrick, E.L. Kilpatrick, Optimizing high-resolution mass spectrometry for the identification of low-abundance post-translational modifications of intact proteins, J. Proteome Res. 16 (2017) 3255–3265.
[33] J.A. Loo, Electrospray ionization mass spectrometry: a technology for studying noncovalent macromolecular complexes, Mass Spectrom. Rev. 16 (1998) 1–23.

[34] G.R. Hilton, J.L. Benesch, Two decades of studying non-covalent biomolecular assemblies by means of electrospray ionization mass spectrometry, J. R. Soc. Interface 9 (2012) 801–816.
[35] G. Young, N. Hundt, D. Cole, A. Fineberg, J. Andrecka, A. Tyler, A. Olerinyova, A. Ansari, E.G. Marklund, M.P. Collier, S.A. Chandler, O. Tkachenko, J. Allen, M. Crispin, N. Billington, Y. Takagi, J.R. Sellers, C. Eichmann, P. Selenko, L. Frey, et al., Quantitative mass imaging of single biological macromolecules, Science 360 (2018) 423–427.
[36] F. Soltermann, E.D.B. Foley, V. Pagnoni, M. Galpin, J.L.P. Benesch, P. Kukura, W. B. Struwe, Quantifying Protein–Protein Interactions by Molecular Counting with Mass Photometry 59, 2020, pp. 10774–10779.
[37] L.P. Lauridsen, A.H. Laustsen, B. Lomonte, J.M. Gutiérrez, Exploring the venom of the forest cobra snake: Toxicovenomics and antivenom profiling of Naja melanoleuca, J. Proteomics 150 (2017) 98–108.
[38] R. Shine, W.R. Branch, J.K. Webb, P.S. Harlow, T. Shine, J.S. Keogh, Ecology of cobras from southern Africa, J. Zool. 272 (2007) 183–193.
[39] G.T.T. Nguyen, C. O'Brien, Y. Wouters, L. Seneci, A. Gallissa-Calzado, I. Campos-Pinto, S. Ahmadi, A.H. Laustsen, A. Ljungars, High-throughput proteomics and in vitro functional characterization of the 26 medically most important elapids and vipers from sub-Saharan Africa, Gigascience 11 (2022) 1–15.
[40] M.G. Grabherr, B.J. Haas, M. Yassour, J.Z. Levin, D.A. Thompson, I. Amit, X. Adiconis, L. Fan, R. Raychowdhury, Q. Zeng, Z. Chen, E. Mauceli, N. Hacohen, A. Gnirke, N. Rhind, F. di Palma, B.W. Birren, C. Nusbaum, K. Lindblad-Toh, N. Friedman, A. Regev, Full-length transcriptome assembly from RNA-Seq data without a reference genome, Nat. Biotechnol. 29 (2011) 644–652.
[41] B.J. Haas. https://github.com/TransDecoder/TransDecoder, 2024.
[42] C. Camacho, G. Coulouris, V. Avagyan, N. Ma, J. Papadopoulos, K. Bealer, T. L. Madden, BLAST+: architecture and applications, BMC Bioinformatics 10 (2009) 1–9.
[43] N.J. Anthis, G.M. Clore, Sequence-specific determination of protein and peptide concentrations by absorbance at 205 nm, Protein Sci. 22 (2013) 851–858.
[44] O.T. Olaoba, P. Karina Dos Santos, H.S. Selistre-de-Araujo, D.H. Ferreira de Souza, Snake venom metalloproteinases (SVMPs): a structure-function update, Toxicon X 7 (2020) 1–15.
[45] K. Ning, D. Fermin, A.I. Nesvizhskii, Comparative analysis of different label-free mass spectrometry based protein abundance estimates and their correlation with RNA-Seq gene expression data, J. Proteome Res. 11 (2012) 2261–2271.
[46] D.H. Lundgren, S.I. Hwang, L. Wu, D.K. Han, Role of spectral counting in quantitative proteomics, Expert Rev. Proteomics 7 (2010) 39–53.
[47] M.A. Bittenbinder, C.N. Zdenek, B. Op den Brouw, N.J. Youngman, J.S. Dobson, A. Naude, F.J. Vonk, B.G. Fry, Coagulotoxic cobras: clinical implications of strong anticoagulant actions of African spitting Naja venoms that are not neutralised by antivenom but are by LY315920 (Varespladib), Toxins (Basel) 10 (2018) 1–11.
[48] A. Ghazalpour, B. Bennett, V.A. Petyuk, L. Orozco, R. Hagopian, I.N. Mungrue, C. R. Farber, J. Sinsheimer, H.M. Kang, N. Furlotte, C.C. Park, P.Z. Wen, H. Brewer, K. Weitz, D.G. Camp 2nd, C. Pan, R. Yordanova, I. Neuhaus, C. Tilford, N. Siemers, P. Gargalovic, E. Eskin, T. Kirchgessner, D.J. Smith, R.D. Smith, A.J. Lusis, Comparative analysis of proteome and transcriptome variation in mouse, PLoS Genet. 7 (2011) 1–17.
[49] M.J. Margres, J.J. McGivern, K.P. Wray, M. Seavy, K. Calvin, D.R. Rokyta, Linking the transcriptome and proteome to characterize the venom of the eastern diamondback rattlesnake (Crotalus adamanteus), J. Proteomics 96 (2014) 145–158.
[50] N.H. Tan, K.Y. Wong, C.H. Tan, Venomics of Naja sputatrix, the Javan spitting cobra: a short neurotoxin-driven venom needing improved antivenom neutralization, J. Proteomics 157 (2017) 18–32.
[51] B. Kalita, S. Singh, A. Patra, A.K. Mukherjee, Quantitative proteomic analysis and antivenom study revealing that neurotoxic phospholipase a(2) enzymes, the major toxin class of Russell's viper venom from southern India, shows the least immuno-recognition and neutralization by commercial polyvalent antivenom, Int. J. Biol. Macromol. 118 (2018) 375–385.
[52] G. Wang, R.N. de Jong, E.T.J. van den Bremer, P. Parren, A.J.R. Heck, Enhancing accuracy in molecular weight determination of highly heterogeneously glycosylated proteins by native tandem mass spectrometry, Anal. Chem. 89 (2017) 4793–4797.
[53] C.W. Vogel, D.C. Fritzinger, Cobra venom factor: structure, function, and humanization for therapeutic complement depletion, Toxicon 56 (2010) 1198–1222.
[54] S.M. Serrano, The long road of research on snake venom serine proteinases, Toxicon 62 (2013) 19–26.
[55] C. Guo, S. Liu, Y. Yao, Q. Zhang, M.Z. Sun, Past decade study of snake venom L-amino acid oxidase, Toxicon 60 (2012) 302–311.
[56] C. Bras-Costa, A.F.A. Chaves, D. Cajado-Carvalho, D. da Silva Pires, D. Andrade-Silva, S.M.T. Serrano, Profilings of subproteomes of lectin-binding proteins of nine Bothrops venoms reveal variability driven by different glycan types, Biochim. Biophys. Acta, Proteins Proteomics 1870 (2022) 1–15.
[57] I.H. Tsai, Y.M. Wang, K.F. Huang, Effects of single N-glycosylation site knockout on folding and defibrinogenating activities of acutobin recombinants from HEK293T, Toxicon 94 (2015) 50–59.
[58] Y.M. Wang, I.H. Tsai, J.M. Chen, A.C. Cheng, K.H. Khoo, Correlation between the glycan variations and defibrinogenating activities of acutobin and its recombinant glycoforms, PloS One 9 (2014) 1–11.
[59] Refeyn. https://www.refeyn.com/post/benefits-and-limitations-of-mass-photometry (accessed 2023-07-27).
[60] D. Cole, G. Young, A. Weigel, A. Sebesta, P. Kukura, Label-free single-molecule imaging with numerical-aperture-shaped interferometric scattering microscopy, ACS Photonics 4 (2017) 211–216.